

Adaptive integration of local region information to detect fine-scale brain activity patterns

ZHEN ZongLei¹, TIAN Jie^{1,2†} & ZHANG Hui¹

¹ Medical Image Processing Group, Key Laboratory of Complex Systems and Intelligence Science, Institute of Automation, Chinese Academy of Sciences, Beijing 100080, China;

² Graduate University of the Chinese Academy of Sciences, Beijing 100039, China

With the rapid development of functional magnetic resonance imaging (fMRI) technology, the spatial resolution of fMRI data is continuously growing. This provides us the possibility to detect the fine-scale patterns of brain activities. The established univariate and multivariate methods to analyze fMRI data mostly focus on detecting the activation blobs without considering the distributed fine-scale patterns within the blobs. To improve the sensitivity of the activation detection, in this paper, multivariate statistical method and univariate statistical method are combined to discover the fine-grained activity patterns. For one voxel in the brain, a local homogenous region is constructed. Then, time courses from the local homogenous region are integrated with multivariate statistical method. Univariate statistical method is finally used to construct the interests of statistic for that voxel. The approach has explicitly taken into account the structures of both activity patterns and existing noise of local brain regions. Therefore, it could highlight the fine-scale activity patterns of the local regions. Experiments with simulated and real fMRI data demonstrate that the proposed method dramatically increases the sensitivity of detection of fine-scale brain activity patterns which contain the subtle information about experimental conditions.

functional magnetic resonance imaging (fMRI), principal component analysis, general linear model, local region, fine-scale activity patterns

Functional magnetic resonance imaging (fMRI) has become a powerful tool for the research into human brain function due to its noninvasiveness and high spatiotemporal resolution. The most popular fMRI technique is blood oxygenation level-dependent (BOLD) fMRI which reflects neural

Received April 2, 2007; accepted June 30, 2007; published online September 10, 2008

doi: 10.1007/s11431-008-0124-7

[†]Corresponding author (email: tian@ieee.org)

Supported by Chair Professors of Changjiang Scholars Program and CAS Hundred Talents Program, National Program on Key Basic Research Projects (Grant No. 2006CB705700), National High-Tech R&D Program of China (Grant No.2006AA04Z216), National Key Technology R&D Program (Grant No. 2006BAH02A25), Joint Research Fund for Overseas Chinese Young Scholars (Grant No.30528027), National Natural Science Foundation of China (Grant Nos.30600151, 30500131 and 60532050), and Natural Science Foundation of Beijing (Grant Nos. 4051002 and 4071003)

activity by mapping of local changes of cerebral blood flow and oxygenation level^[1,2]. Unfortunately, changes in BOLD signal during brain activation are very small (~1%–5%) and are often contaminated by various artifacts. The artifacts are mainly from physiological and physical sources such as pulsatile motion of the brain caused by cardiac cycles, local modulation of the static magnetic field by respiratory movement, subject motion, and white noise. The complicated structure of fMRI signals presents a formidable challenge to detection of the activation patterns of the brain^[3,4].

A variety of methods have been proposed for detecting spatiotemporal patterns of brain activity, and they can be classified into two categories: univariate methods and multivariate methods. As a typical univariate method, the general linear model (GLM) has been widely applied in fMRI data analysis^[5,6]. GLM identifies the activated voxels that are highly correlated to a reference model which characterizes signal changes induced by brain activation. To increase the signal to noise ratio (SNR) and statistical power, GLM heavily relies on spatial smoothing of the data with Gaussian kernel (GK)^[7]. Spatial smoothing is a process by which spatial data points are averaged with their neighbors in the volume. The optimal smoothing depends on the shape of the activation regions and the response distribution of voxels, all of which may not be matched by a standard GK. As a result, the spatial smoothing degrades the native resolution of the data, and the fine-scale patterns of weak effects that characterize neuroscientifically relevant information are blurred or discarded^[8,9].

Various multivariate methods such as principal component analysis (PCA) and independent component analysis (ICA) have been used in fMRI data analysis as well^[10–15]. However, multivariate methods for fMRI data analysis always suffer from a common problem of being crudely applied on the whole brain data, and it is hard for them to detect the fine-scale brain activations due to the fact that the small quantity of activation voxels, especially those with weak response, is usually submerged by the spatiotemporally varying artifacts across the whole brain. In addition, owing to the complicated components of fMRI data, multivariate decomposition of the whole brain data will generally identify a large collection of intrinsic structures (components); it is difficult for researchers to establish a direct correspondence between the identified components and the experiment hypotheses.

In nature, BOLD contrast arises mainly from oxygenation changes in small venules lying close to the site of neuronal activity in spatially extended neuronal ensembles^[16]. The heterogeneity of the brain anatomy determines that the morphology of functional structures is inhomogeneous. To deal with these intrinsic inhomogeneities across the whole brain and discover the underlying fine-grained activity patterns in local brain regions, we propose to combine multivariate statistical method and univariate statistical method to detect brain activations. In our method, for every voxel in the brain, a local homogenous region is firstly constructed. Then, time courses from the local homogenous region are integrated with multivariate statistical method. Finally, univariate statistical method is used to construct the interests of statistic for that voxel. Specifically, PCA and GLM are adopted in our multivariate and univariate analysis steps, respectively. For convenience, we refer to our method as LPCA-GLM across the paper. For the LPCA-GLM framework, PCA can be regarded as a spatiotemporal filter adapted to the local regions. If a voxel has a low SNR, its neighboring voxels will provide more information to estimate the stimulation effects for it. This spatial integration naturally derives from an automatic way driven by the underlying spatiotemporal activity of the local regions. Thus, unlike GK smoothing or global multivariate analysis, LPCA-GLM can adaptively integrate information from the local brain regions and highlight more

fine-scale brain activity patterns.

1 General description of the LPCA-GLM

Figure 1 graphically illustrates the principle of LPCA-GLM approach. The detailed procedure of LPCA-GLM is described as follows:

(1) For a specific voxel v_i , a local homogeneous region R_i is firstly grouped by region growing method which adopts v_i as the seed. We use the region growing method rather than a fixed regular window to confine the homogeneous regions because the activity regions of brain are irregular. To some extent, the region growing method can adapt the shape of local spatial structures of the brain activity and help us to detect fine-scale brain activity patterns.

(2) The time courses from the local region R_i are decomposed to different components with PCA^[17], and then some pairs of spatial and temporal modes are acquired from the decomposition. As alternatives to PCA, other multivariate methods such as ICA^[11], multivariate linear model (MLM)^[18] and partial least square (PLS)^[19] can be easily incorporated into our framework.

(3) GLM is used to model the expected task-related time courses with the temporal modes of the components from the PCA decomposition. Spatial modes are weighted by the significant regression coefficients ($p < 0.05$) to form the combined spatial modes for GLM. The combined spatial modes represent the estimate of activity of multiple voxels involved in the task for that local region.

(4) Statistical parameter of the voxel v_i is obtained from LPCA-GLM analysis. As R_i moves throughout the brain, statistical parameters are computed for each voxel, and a continuous map is obtained.

(5) Statistical inference is performed by the nonparametric permutation to acquire the significant activation voxels related to particular conditions.

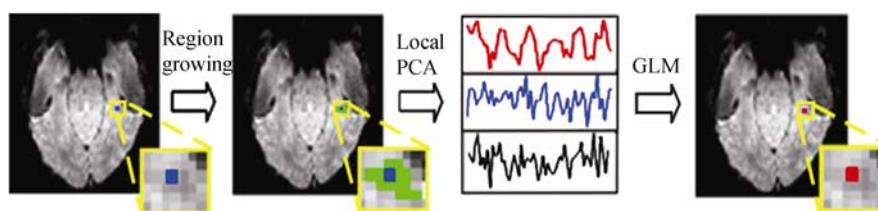


Figure 1 Principle of LPCA-GLM method for fMRI activation detection.

2 Finding homogeneous brain regions

Despite the diverse morphology of functional structures, brain activation is more likely to occur in clusters of spatially connected voxels than isolated voxels^[20–22]. Based on this knowledge, region growing method was introduced to find the local homogeneous regions^[23–25]. The goal of the algorithm is to group a set of voxels on the brain cortex into a region R that is homogeneous. Starting with a seed voxel, the region growing method iteratively groups voxels by merging neighboring voxels whose time course has maximum correlation with the current region. Assuming voxel v_i is specified as the initial seed of local region R_i , and the homogeneous region is $R_{i,n-1}$ after the $n-1$ -th iteration, the neighborhood of the region R_i can be defined as

$$E = \{q \in R_{i,n-1} \mid N(q) \cap R_{i,n-1} \neq \emptyset\}$$

where $N(q)$ denotes the standard 8- or 26-connexity neighborhood for voxel q .

At step n , the voxel p is added to region R_i if it satisfies the following similarity criterion:

$$p = \arg \max_{p \in E} \left(\frac{1}{\#R_{i,n-1}} \sum_{w \in R_i} \text{corr}(y_p, y_w) \right),$$

where $\#R_{i,n-1}$ is the number of voxels in region $R_{i,n-1}$, corr is Pearson linear correlation, and y_p and y_w are the time series of voxels p and w . This grown procedure is repeated until the size of the region reaches a predefined critical value N . Therefore, a local homogenous region R_i for voxel v_i is obtained by region growing as illustrated in Figure 2.

The size of local region is an important parameter for us to combine multivariate and univariate analyses. Depending on the region size, the effect of local multivariate analysis will behave differently. For a very small local region, the effect is limited because the local multivariate analysis can rely on few voxels. For a very large local region, the local region will be too heterogeneous and the drawback of the global multivariate analysis will recur.

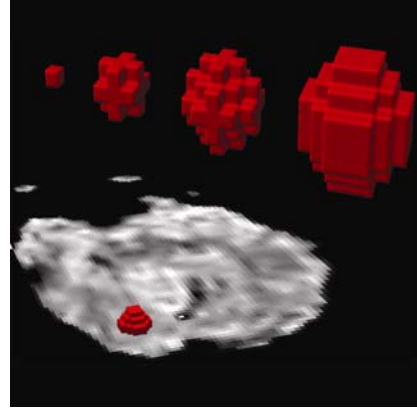


Figure 2 Local homogeneous regions with various sizes generated by region growing method.

3 Combining PCA and GLM to detect fine-scale activations

The time series from local region R_i can be organized as an $N \times P$ matrix \mathbf{Y} with rows corresponding to the voxels in R_i , and columns to the samples (scans). The $N \times N$ dimension sample covariance matrices $\mathbf{Y}\mathbf{Y}^T$ reports directly the local spatial covariance structure. PCA, which is generally implemented by singular value decomposition (SVD), can find the eigenvalues and eigenvector of the covariance matrix of \mathbf{Y} and decompose \mathbf{Y} into pairs of spatial and temporal modes:

$$\mathbf{Y} = \mathbf{U}\mathbf{L}\mathbf{W}^T = \sum_{k=1}^N l_k^{1/2} \mathbf{u}_k \mathbf{w}_k^T.$$

The spatial mode \mathbf{u}_k , which is $N \times 1$ orthogonal principal eigenvectors of $\mathbf{Y}\mathbf{Y}^T$, represents the spatial patterns in the local region. The temporal mode \mathbf{w}_k , which is $P \times 1$ orthogonal principal eigenvectors of $\mathbf{Y}^T\mathbf{Y}$, indicates the temporal profile of the corresponding spatial pattern \mathbf{u}_k . The eigenvalues of the covariance matrix $\mathbf{Y}\mathbf{Y}^T$ l_k give the component variance explained by \mathbf{u}_k and \mathbf{w}_k . Generally, distinct condition effects are captured by different components after the decomposition of data in the local regions.

GLM is used to model the expected task-related time courses of the temporal modes from PCA decomposition. We estimate the response amplitude in the local region as a least-squares fit of the predictor time course for each condition from components that account for the first cumulative 80% of the data variance for each local region:

$$\mathbf{w}_k = \boldsymbol{\beta}_k \mathbf{X} + \boldsymbol{\varepsilon}.$$

Spatial modes \mathbf{u}_k with the corresponding temporal modes \mathbf{w}_k which contribute to the multiple regression models significantly ($p < 0.05$ for its regression coefficient) are weighted by the regression coefficients $\boldsymbol{\beta}_k$ to form the combined spatial mode. The combined spatial mode demonstrates the

estimated activity of multiple voxels involved in experimental conditions for that local region. The parameter of combined spatial mode at the seed voxel v_i will be used as the statistic of condition effects for that voxel. As R_i moves throughout the brain, statistical parameter maps are constructed. Statistical inference can be carried out on the parameter maps to discover the significant activation voxels related to particular conditions. Note that when doing PCA in local regions, principal components are defined on an arbitrary sign. Consequently, GLM computed on the principal components will result in a positive or negative β value. To avoid this effect, the absolute value of β is used in the statistical inference. Therefore, p maps represent the local brain regions that are mostly different in conditions regardless of the activity relatively increasing or decreasing.

4 Optimal filtering

Proper noise estimation and elimination are essential for the detection of weak signal evoked by the experimental stimulus. The application of PCA on the local homogeneous regions can improve SNR significantly due to the joint implication of multiple voxels. In contrast to the 'hard' averaging of voxel time courses within a local region as GK smoothing does, the principal component time-course profiles reflect a data-led, intelligent averaging, $\mathbf{w}_k \propto \mathbf{Y}^T \mathbf{u}_k$, which is equivalent to recovering the interests of signals contained in the local region with the best spatiotemporal filter. The voxelwise weights applied to the individual row vectors of the data matrix \mathbf{Y} are determined by the corresponding spatial distribution of the eigenimages \mathbf{u}_k . Likewise, the spatial distribution of \mathbf{u}_k comprising the eigenimages are computed as appropriately weighted temporal averages $\mathbf{u}_k \propto \mathbf{Y} \mathbf{w}_k$, thereby reducing the variability induced by the noise. In short, this local data-led adaptive multi-variate method can provide substantial SNR ratio improvement and will make the activation detection more precise, especially when the actual activation signal is weak.

5 Data description and experimental paradigms

5.1 Simulated data

A two-condition slow event-related experiment was simulated. Each event lasted 500 ms and their onsets were separated by 16 s. The condition order was random, and there were 30 events per condition. The time course of fMRI signal associated with each condition was simulated by convolving each event with the canonical hemodynamic response function (HRF)^[26]. The parameters of the functional volume are as follows: number of slice =5, voxel sizes=3 mm×3 mm×3 mm, TR=2000 ms and matrix=64×64. Five active regions with different shapes and varied sizes (10, 30, 90, 180 and 270 voxels, respectively) were generated. Each condition was associated with a Gaussian white-noise effect pattern within the active regions and no effects outside the regions. Gaussian white noises as the effect patterns ensured the effects power distributed among all the spatial-frequency bands. Consequently, the condition information was contained both in their locally averaged components (low frequency) and in their spatial fine structures (high frequency). The effect signals were added to spatiotemporal noise generated by slightly spatial smoothing of Gaussian white noise with a GK of 3.5 mm full width at half maximum (FWHM) to imitate the correlation found between the residual time courses of neighboring voxels in real fMRI data. Five datasets were generated with different functional contrast-to-noise ratio (CNR) levels (0.2, 0.4, 0.6,

0.8, and 1.0). The CNR was defined as the spatial average within the effect-region of the absolute activity level at the maximum of the hemodynamic response divided by the temporal standard deviation of the background noise^[27].

5.2 Real fMRI data

5.2.1 Visual experiment. The experimental data were from a 250-s experimental session consisting of ten epochs with stimulus onset asynchrony of 25 s. An 8-Hz flickering checkerboard stimulus was presented to subjects for 3 s at the beginning of each epoch. Details of this experimental design can be found in Duann et al.^[14]. A 3T Bruker Medspec 30/100 scanner was used to acquire the functional images with a gradient-echo EPI sequence (TR/TE=500/70 ms, flip angle=90°, matrix=64×64, FOV=250 mm×250 mm, slice thickness = 5 mm with 2 mm gap). Five contiguous axial slices were scanned, and the visual cortex was mainly covered. T1-weighted images (matrix = 256×256, FOV =250 mm×250 mm) with the same slice position as the functional images were also acquired. The data of this experiment is available as a part of the FMRLAB toolbox for fMRI ICA analysis^[14].

5.2.2 Finger tapping experiment. A simple finger tapping task was conducted on a right-handed subject with normal vision. The experiment paradigm was a conventional 30 s block design, alternated by rest and task of finger tapping. Subject was visually cued to perform bimanual finger tapping with the index fingers at 2 Hz. The control task consisted of viewing a fixation cross (without tapping) displayed on a screen. MR imaging was taken on a 3T Siemens Trio whole body scanner at Beijing Tiantan Hospital. Functional data were acquired by a T2*-weighted single-shot gradient-echo EPI sequence (TR/TE= 2000/30 ms, flip angle = 90°, matrix = 64×64, FOV= 200 mm×200 mm, 27 contiguous axial slices, slice thickness = 3 mm) for 240 volumes per subject. A set of T1-weighted structural images with the same slice position as the functional images (matrix = 256×256, FOV = 256 mm×256 mm, in-plane resolution = 1 mm×1 mm) were acquired prior to functional scans.

6 Results

6.1 Simulated data analysis

The simulated data were analyzed in three ways: GLM with no smoothing (GLM), GLM with GK (GK-GLM), and LPCA-GLM method. Two GK with FWHM of 6 mm and 9 mm were used separately to smooth the data. There are two widely used GK in fMRI data analysis. For comparison, two local regions with 10 and 30 voxels were adopted in LPCA-GLM method to approximately match the range of spatial combination of signals between GK-GLM and LPCA-GLM approaches.

Receiver operating characteristic (ROC) analysis was conducted on the simulated data for the quantitative evaluation of three different analyses^[28,29]. An ROC curve is the plot of true activation rate versus false activation rate for the threshold varying over the complete range of map values.

True activation rate (sensitivity) is the ratio of the number of voxels correctly identified as the activation to the total number of truly activated voxels.

False activation rate (1-specificity) is the ratio of the number of voxels incorrectly identified as activated to the total number of truly non-activated voxels.

ROC shows the tradeoff relationship between sensitivity and specificity of the activation

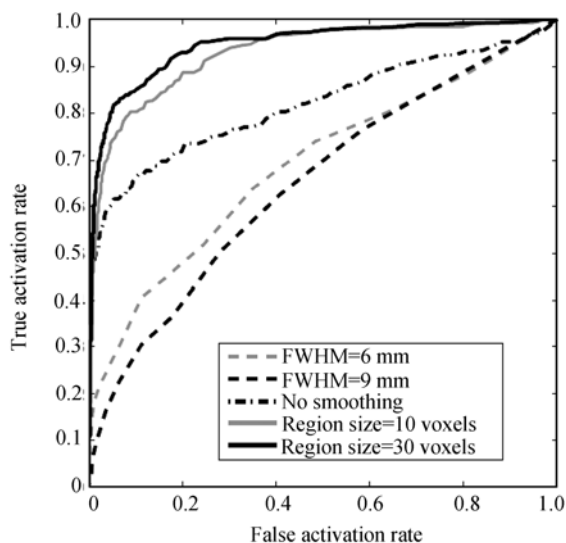


Figure 3 ROC curves for one special case of simulated data with CNR being 0.4.

performs worse than LPCA-GLM approach, but better than the GK-GLM. This reflects the fact that effects in our simulation are equally strong in all spatial-frequency bands up to the Nyquist limit imposed by voxel size. GK-GLM cannot detect the high frequency fine-scale patterns because GK has filtered out the high spatial-frequency component of the effect patterns. However, LPCA-GLM can effectively employ the local distributed spatial patterns in all frequency components to discriminate the effect under different conditions.

Figure 4 shows the AUC for each analysis plotted as functions of CNR. It is clear that smoothing degrades performance of the GK-GLM under every CNR. The more the smoothing is, the worse the performance will be because GK smoothing fails to benefit from local spatial combination of signals. LPCA-GLM performs much better than GLM and GK-GLM for all situations, benefiting from spatial multivariate integration in the local region.

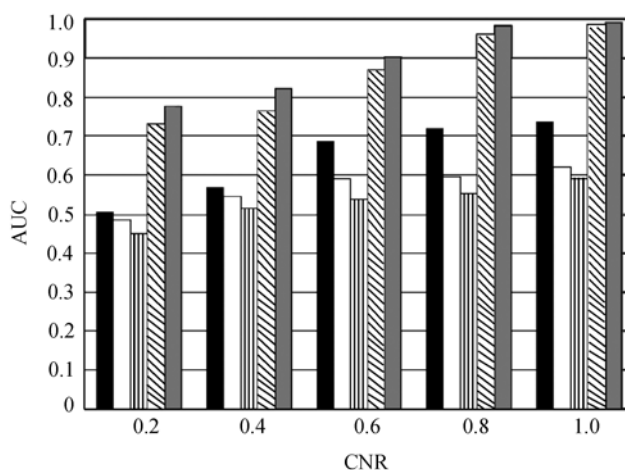


Figure 4 Areas under ROC for GLM, GK-GLM and LPCA-GLM at various CNR, averaged over 30 simulations. At every CNR, from left to right, the five bars represent the AUC from GLM with no smoothing, GLM with FWHM=6 mm, GLM with FWHM=9 mm, LPCA-GLM with region size = 10 voxels, LPCA-GLM with region size = 30 voxels, respectively.

detection methods. Thus, it provides a way to compare the performance of different analyses quantitatively. Furthermore, the area under ROC (AUC) represents a summary measure of what extent of high sensitivity and specificity can be simultaneously achieved. Concretely, AUC indicates how well a given statistic distinguishes between effect-regions and pure noise in our simulations.

Figure 3 illustrates the ROC curves of different analyses for one particular case of the simulated data with CNR being 0.4. It can be observed that the ROC curves of LPCA-GLM approach the top left corner primarily, above the curves of GLM and GK-GLM. With no smoothing, GLM performs

6.2 Real data analysis

All data were preprocessed using SPM2 (<http://www.fil.ion.ucl.ac.uk/SPM/>)^[5,6] as follows. Slices were temporally realigned to compensate for the acquisition time lag. Whole volume images were realigned to compensate for the head movement, and drifts were corrected by second-order polynomial detrending. The data from two experiments were analyzed by both GK-GLM and LPCA-GLM. As seen from the simulation experiment, LPCA-GLM performs better when the local region size is 30 voxels. We hereby set the local region size as 30 voxels in the analysis of real fMRI data with LPCA-GLM. A GK of FWHM equal to 9 mm was used in the GK-GLM analysis to approximately match the range of spatial combination of signals between LPCA-GLM and GK-GLM analyses. The statistical inferences were performed by a permutation test. 1000 independent permutations were realized to determine the p maps for every condition^[30,31]. To obtain an inferential map accounting for multiple comparisons, all p maps from the randomization were thresholded to ensure the average FDR to be less than $q=0.05$ ^[32].

6.2.1 Visual experiment. Both GK-GLM and LPCA-GLM analyses returned the activation regions which extended from the centrally located main blood supply vessels to the primary visual cortex as shown in Figure 5. It is clear that GK smoothing enhances the statistical power at the expense of spatial resolution (Figure 5(a)). However, LPCA-GLM analysis with a local region containing the matching size of GK localizes the activations while efficiently preserving fine structures of local regions as displayed in Figure 5(b). With GK smoothing, the fine-scale patterns were blurred due to the mismatch between shape of GK and spatial distribution of activation voxels within the local regions. In contrast, application of PCA on the local homogeneous regions is equivalent to a data-driven spatiotemporal filter as discussed in section 4. By adaptively integrating the information of multiple voxels in the local regions, this local data-led multivariate decomposition provides a substantial SNR improvement and makes the activation detection with the LPCA-GLM more precise, especially for the voxels with weak responses.

6.2.2 Finger tapping experiment. Figure 6 illustrates the activation maps from GK-GLM and LPCA-GLM analyses. As expected, both GK-GLM and LPCA-GLM can find the major blobs such as the primary motor cortex, supplementary motor area, premotor cortex, and cerebellum (not shown in Figure 6). Smoothing data with GK of FWHM =9 mm resulted in clean maps and foci regions of activations (Figure 6(a)). However, it was noted that fine-scale information was lost. For example, due to the inappropriate smoothing, the primary motor and premotor cortex were merged as one big activation region. In contrast to GK-GLM, LPCA-GLM with local region size of 30 voxels that closely matched the size of GK of FWHM=9 mm was better for detecting the activation voxels with the higher spatial resolution (Figure 6(b)). The primary motor area and premotor area were easily distinguished from each other as presented in Figure 6(b). In addition to the activation regions detected by GK-GLM, LPCA-GLM discovered some fine-scale activation blobs at parieto-frontal regions which might involve motion plan. GK-GLM failed to detect these regions because the fine-scale information was lost when data were smoothed by GK. The results demonstrate that there are many voxels containing weak effects related to experiment conditions in the local regions. LPCA-GLM method adaptively integrates the information of the task-related activation from the local regions. Therefore, it can consistently detect these activation voxels.

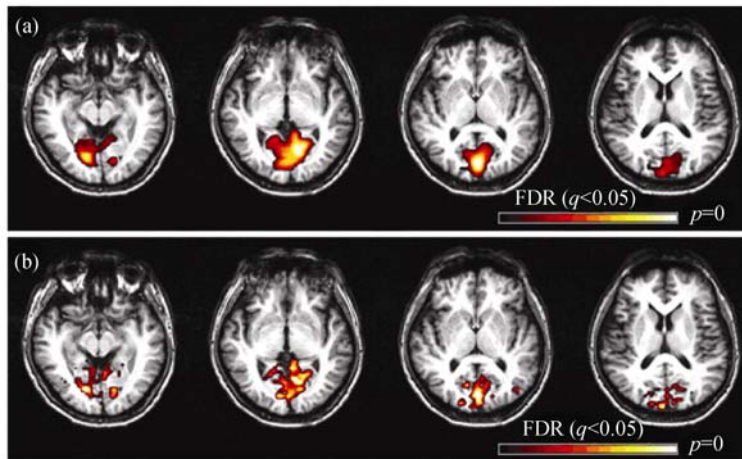


Figure 5 Activation maps for visual experiment, obtained by GK-GLM and LPCA-GLM analyses. (a) Maps from GK-GLM with GK of FWHM=9 mm spatial smoothing; (b) maps from LPCA-GLM with local region size of 30 voxels.

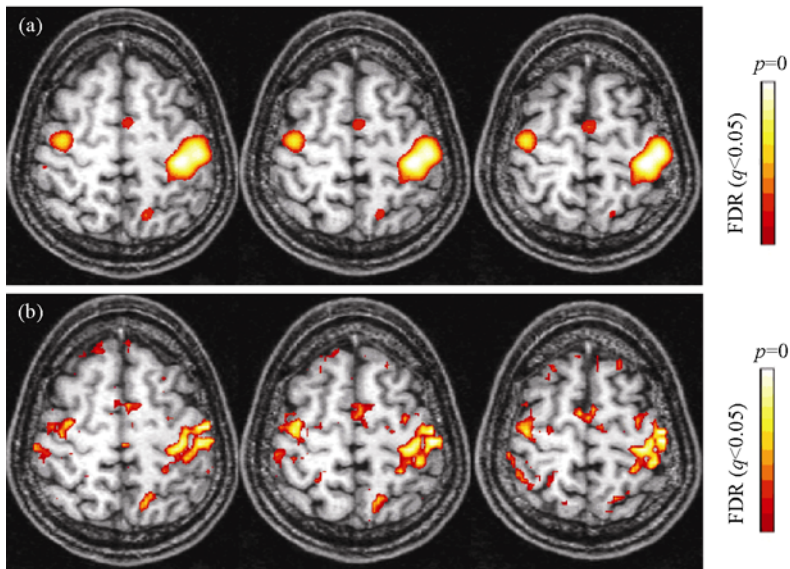


Figure 6 Activation maps for finger tapping experiment, obtained by GK-GLM and LPCA-GLM analyses. (a) Maps from GK-GLM with GK of FWHM=9 mm spatial smoothing; (b) maps from LPCA-GLM with local region size of 30 voxels.

7 Conclusions

The activity of functional activation clusters is fundamentally heterogeneous. Smoothing the data with spatially invariant GK degrades anatomic boundaries and distorts the underlying spatiotemporal signals of brain activity. Adaptively integrating the information presented in the local region is vital to deal with these intrinsic inhomogeneities across the brain regions and discover the underlying fine-grained activity patterns related to the experimental stimulus. In this paper, the LPCA-GLM method was proposed to detect the fine-scale activity patterns contained in the local regions. Compared to GK spatial smoothing, LPCA can better adapt to the inherent spatial variability of the functional signals in the local homogenous regions. Therefore, LPCA-GLM can well localize the activations while efficiently preserving the fine-scale activity patterns, especially for

those voxels with weak responses. Experiments with simulated and real fMRI data demonstrate that LPCA-GLM can dramatically increase the sensitivity on the detection of fine-scale brain activity patterns which contain subtle information about the experimental conditions.

- 1 Ogawa S, Lee T, Kay A, et al. Brain magnetic resonance imaging with contrast dependent on blood oxygenation. *Proc Natl Acad Sci USA*, 1990, 87(24): 9868–9872[[DOI](#)]
- 2 Kwong K, Belliveau J, Chesler D, et al. Dynamic magnetic resonance imaging of human brain activity during primary sensory stimulation. *Proc Natl Acad Sci USA*, 1992, 89(12): 5675–5679[[DOI](#)]
- 3 Petersson K, Nichols T, Poline J, et al. Statistical limitations in functional neuroimaging I. non-inferential methods and statistical models. *Philos Trans R Soc Lond B Biol Sci*, 1999, 354(1387): 1240–1260
- 4 Petersson K, Nichols T, Poline J, et al. Statistical limitations in functional neuroimaging II, signal detection and statistical inference. *Philos Trans R Soc Lond B Biol Sci*, 1999, 354(1387): 1261–1281[[DOI](#)]
- 5 Friston K, Holmes A, Worsley K, et al. Statistical parametric maps in functional imaging: A general linear approach. *Hum Brain Mapp*, 1995, 2(4): 189–210[[DOI](#)]
- 6 Friston K, Holmes A, Poline J, et al. Analysis of fMRI time-series revisited. *NeuroImage*, 1995, 2(1): 45–53[[DOI](#)]
- 7 Friston K, Josephs O, Zarahn E, et al. To smooth or not to smooth? Bias and efficiency in fMRI time-series analysis. *NeuroImage*, 2000, 12(2): 196–208[[DOI](#)]
- 8 Kriegeskorte N, Goebel R, Bandettini P. Information-based functional brain mapping. *Proc Natl Acad Sci USA*, 2006, 103(10): 3863–3868[[DOI](#)]
- 9 Bandettini P. Functional MRI today. *Int J Psychophysiol*, 2007, 63(2): 138–145[[DOI](#)]
- 10 Friston K, Frith C, Liddle P, et al. Functional connectivity: The principal component analysis of large (PET) data sets. *J Cereb Blood Flow Metab*, 1993, 13(1): 5–14
- 11 McKeown M, Makeig S, Brown G, et al. Analysis of fMRI data by blind separation into independent spatial components. *Hum Brain Mapp*, 1998, 6(3): 160–188
- 12 Formisano E, Esposito F, Kriegeskorte N, et al. Spatial independent component analysis of functional magnetic resonance imaging time-series: characterization of the cortical components. *Neurocomputing*, 2002, 49(1-4): 241–254[[DOI](#)]
- 13 Calhoun V, Adali T, Pearlson G, et al. Spatial and temporal independent component analysis of functional MRI data containing a pair of task-related waveforms. *Hum Brain Mapp*, 2001, 13(1): 43–53[[DOI](#)]
- 14 Duann J, Jung T, Kuo W, et al. Single-trial variability in event-related BOLD signals. *NeuroImage*, 2002, 15(4): 823–835[[DOI](#)]
- 15 Strother S, Anderson J, Hansen L, et al. The quantitative evaluation of functional neuroimaging experiments: the NPAIRS data analysis framework. *NeuroImage*, 2002, 15(4): 747–771[[DOI](#)]
- 16 Turner R. How much cortex can a vein drain? Down stream dilution of activation-related cerebral blood oxygenation changes. *NeuroImage*, 2002, 16(4): 1062–1067[[DOI](#)]
- 17 Andersen A H, Gash D M, Avison M J. Principal component analysis of the dynamic response measured by fMRI: A generalized linear systems framework. *Magn Reson Imaging*, 1999, 17(6): 795–815[[DOI](#)]
- 18 Worsley K, Poline J, Friston K, et al. Characterizing the response of PET and fMRI data using multivariate linear models. *NeuroImage*, 1998, 6(4): 305–319[[DOI](#)]
- 19 McIntosh A, Chau W, Protzner A. Spatiotemporal analysis of event-related fMRI data using partial least squares. *NeuroImage*, 2004, 23(2): 764–775[[DOI](#)]
- 20 Tononi G, McIntosh A, Russell D, et al. Functional clustering: identifying strongly interactive brain regions in neuroimaging data. *NeuroImage*, 1998, 7(2): 133–149[[DOI](#)]
- 21 Katanoda K, Matsuda Y, Sugishita M, et al. A spatial-temporal regression model for the analysis of functional MRI data. *NeuroImage*, 2002, 17(3): 1415–1428[[DOI](#)]
- 22 Zang Y, Jiang T, Lu Y, et al. Regional homogeneity approach to fMRI data analysis. *NeuroImage*, 2004, 22(1): 394–400[[DOI](#)]
- 23 Morel J, Solimini S. *Variational Methods in Image Segmentation*. Basel: Birkhauser Publishing, Inc, 1995
- 24 Lu Y, Jiang T, Zang Y, et al. Region growing method for the analysis of functional MRI data. *NeuroImage*, 2003, 20(1): 455–465[[DOI](#)]
- 25 Bellec P, Perlberg V, Jbabdi S, et al. Identification of large-scale networks in the brain using fMRI. *NeuroImage*, 2006, 29(4): 1231–1243[[DOI](#)]
- 26 Friston K J, Fletcher P, Josephs O, et al. Event-related fMRI: characterizing differential responses. *NeuroImage*, 1998, 7(1): 30–40[[DOI](#)]
- 27 Langer N. Tutorial in biostatistics: statistical approaches to human brain mapping by functional magnetic resonance imaging. *Stat Med*, 1996, 15(4): 389–428[[DOI](#)]
- 28 Sorenson J, Wang X. ROC methods for evaluation of fMRI techniques. *Magn Reson Med*, 1996, 36(5): 737–744[[DOI](#)]
- 29 Skudlarski P, Constable R T, Gore J C. ROC analysis of statistical methods used in functional MRI: individual subjects. *NeuroImage*, 1999, 9 (3): 311–329[[DOI](#)]
- 30 Nichols T, Holmes A. Nonparametric permutation tests for functional neuroimaging: a primer with examples. *Hum Brain Mapp*, 2000, 15(1): 1–25[[DOI](#)]
- 31 Efron B, Tibshirani R. *An Introduction to the Bootstrap*. New York: Chapman Hall, 1993. 202–219
- 32 Genovese C, Lazar N, Nichols T. Thresholding of statistical maps in functional neuroimaging using the false discovery rate. *NeuroImage*, 2002, 15(4): 870–878[[DOI](#)]